

On High-Frequency Field Oscillations (>100 Hz) and the Spectral Leakage of Spiking Activity

Robson Scheffer-Teixeira, Hindiael Belchior, Richardson N. Leão, Sidarta Ribeiro, and Adriano B. L. Tort

Brain Institute, Federal University of Rio Grande do Norte, Natal, Rio Grande do Norte 59056, Brazil

Recent reports converge to the idea that high-frequency oscillations in local field potentials (LFPs) represent multiunit activity. In particular, the amplitude of LFP activity above 100 Hz—commonly referred to as “high-gamma” or “epsilon” band—was found to correlate with firing rate. However, other studies suggest the existence of true LFP oscillations at this frequency range that are different from the well established ripple oscillations. Using multisite recordings of the hippocampus of freely moving rats, we show here that high-frequency LFP oscillations can represent either the spectral leakage of spiking activity or a genuine rhythm, depending on recording location. Both spike-leaked, spurious activity and true fast oscillations couple to theta phase; however, the two phenomena can be clearly distinguished by other key features, such as preferred coupling phase and spectral signatures. Our results argue against the idea that all high-frequency LFP activity stems from spike contamination and suggest avoiding defining brain rhythms solely based on frequency range.

Introduction

Over the last 5 years, a growing consensus has emerged that high-frequency activity (>100 Hz) in local field potentials (LFPs) essentially reflects spiking activity (Ray et al., 2008b; Ray et al., 2008c; Jia and Kohn, 2011; Ray and Maunsell, 2011; Belluscio et al., 2012; Buzsáki and Wang, 2012; Buzsáki et al., 2012; see also Manning et al., 2009). This upper part of the LFP spectrum has been called “high-gamma” (Canolty et al., 2006; Ray et al., 2008a; Ray and Maunsell, 2011) or “epsilon” band (Freeman, 2007; Belluscio et al., 2012). Some researchers have stressed the broadband nature of the power changes associated with spiking activity (Manning et al., 2009) and advocated avoiding the term “oscillations” when referring to these phenomena (Jacobs et al., 2010). The evidence that high-frequency LFP activity stems from extracellular spikes is several fold: (1) the power of broadband high-gamma activity correlates well with firing rate (Ray et al., 2008c; Ray and Maunsell, 2011); (2) local increases of high-frequency LFP activity are restricted to cortical regions expected to present increased spiking activity (Miller et al., 2009; Miller, 2010); (3) manually removing extracellular spikes reduces LFP power in high-frequency bands

(Belluscio et al., 2012); and (4) there are typically prominent increases of high-frequency band power in time–frequency decompositions of spike-triggered averages of LFPs (Ray et al., 2008b; Belluscio et al., 2012; see also supporting figures in Colgin et al., 2009; Peyrache et al., 2011).

The notion that the upper LFP spectrum may reflect multiunit activity implies that examining broadband changes in LFP power could be a proxy for tracking neuronal activity (Manning et al., 2009; Buzsáki and Wang, 2012; Buzsáki et al., 2012); this is particularly good news to those interested in brain–machine interfaces (Crone et al., 2006; Miller et al., 2009). The purpose of the present work, however, is to challenge the emerging view of high-frequency LFP activity as essentially denoting spiking activity. Recent work of ours has provided evidence for genuine LFP oscillations above 100 Hz in the hippocampus and neocortex of rodents (Tort et al., 2008; Scheffzük et al., 2011; Scheffer-Teixeira et al., 2012), which we refer to as high-frequency oscillations (HFO). We have previously shown that HFOs differ from sharp wave-associated ripple oscillations (Scheffer-Teixeira et al., 2012), which is to date one of the few well accepted, true oscillatory activities above 100 Hz. Here we use a cross-frequency coupling (CFC) approach (Tort et al., 2010b) to demonstrate that HFOs can be clearly distinguished from contamination of the LFP by multiunit activity. Nevertheless, we also show that extracellular spikes can lead to broadband high-frequency LFP activity as assessed by the same CFC framework. We conclude that LFP activity above 100 Hz can either denote true neuronal oscillations or spike “contamination” (or “leakage”). These results argue against the generalization of fast field activity as mainly reflecting extracellular action potentials.

Materials and Methods

Data analysis. We analyzed three datasets recorded from the CA1 region of freely moving rats (see below, Dataset 1, Dataset 2, Dataset 3). All analyses were performed in MATLAB (MathWorks).

Received Sept. 3, 2012; revised Nov. 22, 2012; accepted Nov. 27, 2012.

Author contributions: A.B.L.T. designed research; R.S.-T., H.B., and R.N.L. performed research; R.S.-T., S.R., and A.B.L.T. analyzed data; R.S.-T., S.R., and A.B.L.T. wrote the paper.

This work was supported by Conselho Nacional de Desenvolvimento Científico e Tecnológico (CNPq), Coordenação de Aperfeiçoamento de Pessoal de Nível Superior (CAPES), and Fundação de Apoio à Pesquisa do Estado do Rio Grande do Norte (FAPERN). We thank the Buzsáki laboratory for making *in vivo* CA1 recordings publicly available through the Collaborative Research in Computational Neuroscience website (<http://crcns.org/>), a data-sharing website funded by the National Science Foundation.

The authors declare no competing financial interests.

Correspondence should be addressed to Dr. Adriano B.L. Tort, Brain Institute, Federal University of Rio Grande do Norte, Rua Nascimento de Castro, 2155 Lagoa Nova, Natal, Rio Grande do Norte 59056-450, Brazil. E-mail: tort@neuro.ufrn.br.

DOI:10.1523/JNEUROSCI.4217-12.2013

Copyright © 2013 the authors 0270-6474/13/331535-05\$15.00/0

Phase-amplitude coupling. To estimate phase-amplitude CFC between two ranges of frequencies of interest, we employed the modulation index (MI) described in detail elsewhere (Tort et al., 2008; Tort et al., 2010b). To obtain the comodulation map, the MI is computed for multiple frequency band pairs (f_p , f_A), and the values are expressed in a bidimensional pseudocolor plot in which warm colors denote the presence of CFC between the phase and the amplitude of the frequencies depicted in the x-axis and y-axis, respectively.

Power spectral analyses, filter settings, and instantaneous phase and amplitude. Power spectra were estimated by means of the Welch method (50% overlapping Hamming windows with a length of 4 s). LFP signals were filtered with a least square linear-phase finite impulse response (FIR) filter using the *eegfilt* function from the EEGLAB Toolbox (Delorme and Makeig, 2004). The Hilbert transform was used to obtain the instantaneous amplitude and phase time series.

Triggered LFP averages. LFP averages were computed using two types of trigger: (1) spike times of multiunit activity; and (2) the peaks of high-frequency oscillations. The first one constitutes the standard spike-triggered average, which was obtained by averaging 500 ms LFP epochs centered on spike times. The second approach involves filtering the LFP signal at the frequency range under study to obtain the timestamps of peak amplitude within theta cycles. The triggered trace is obtained by averaging 500 ms LFP epochs centered at these timestamps.

Dataset 1. We analyzed a dataset from György Buzsáki's Laboratory, which was downloaded from the Collaborative Research in Computational Neuroscience data sharing website (<http://crcns.org/>). The dataset consisted of recordings from the right dorsal CA1 region of the hippocampus using four- or eight-shank multisite probes (200 μ m separation) implanted in three male Long Evans rats. Each shank had eight recording sites (160 μ m² each site; impedance of 1–3 M Ω ; 20 μ m separation) that spanned the pyramidal layer (Mizuseki et al., 2009). Recordings were made while rats explored an open field; signals were amplified (1000 \times), bandpass filtered (1 Hz – 5 kHz), and digitized at 20 kHz (DataMax System, RC Electronics); LFPs were obtained by down-sampling to 1250 Hz; spike times were obtained semiautomatically after high-pass filtering wideband signals at 800 Hz (Mizuseki et al., 2009). Detailed methods are available online at <http://crcns.org/>.

Dataset 2. We also analyzed CA1 recordings obtained from electrodes located at multiple CA1 sites, including sites above the pyramidal layer (Scheffer-Teixeira et al., 2012), in four male Wistar rats freely moving in an open field. Methodological details were previously described in Scheffer-Teixeira et al. (2012). Briefly, rats were chronically implanted with 4 \times 8 multielectrode arrays (Teflon-coated tungsten microwires; diameter, 50 μ m; inter-electrode spacing, 300 μ m; impedance, 0.3 M Ω) targeting the right dorsal hippocampus (centered at: anteroposterior (AP), –3.6 mm from bregma; mediolateral (ML), +1.6 mm; dorsoventral (DV), 2.4 mm from the pial surface). Recordings were performed using a multichannel acquisition processor (Plexon). LFPs were amplified (1000 \times), filtered (0.7–300 Hz), and digitized at 1000 Hz. Spikes were amplified (1000 \times), filtered (300–8000 Hz), and digitized at 40 kHz. Spike sorting was performed offline using a principal component-based algorithm (Offline Sorter, Plexon).

Dataset 3. We recorded from a freely moving male Wistar rat implanted with a 16-site probe across the left CA1 region (NeuroNexus Technologies; site area, 703 μ m²; separation, 100 μ m; impedance, 1–1.5 M Ω ; location, –3.6 mm AP; –2.5 mm ML). Signals were amplified (200 \times), filtered (1–7.5 kHz), and digitized at 25 kHz (RHA2116, Intan Technologies). LFPs were obtained by down-sampling to 2500 Hz. Site

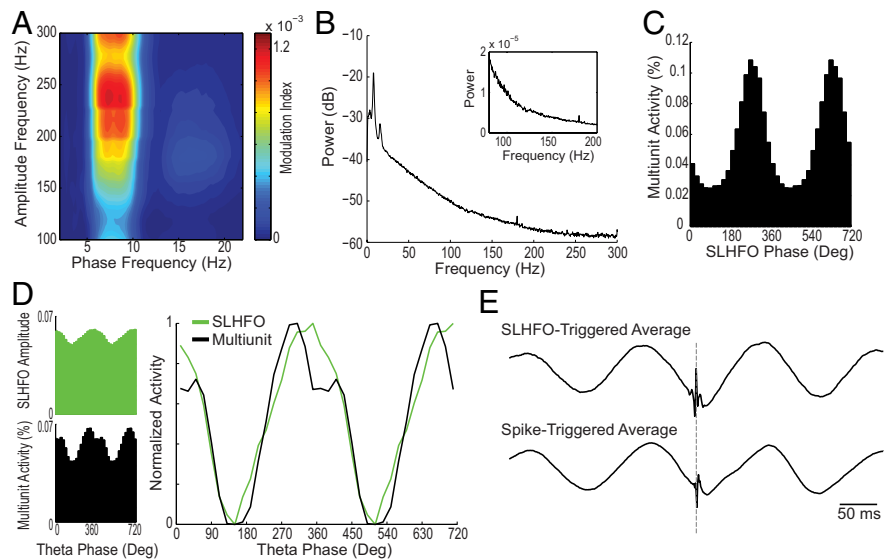


Figure 1. Theta phase modulates broadband high-frequency oscillations >100 Hz in the hippocampus, which correspond to spiking activity. **A**, Comodulation map. Warm colors denote presence of phase–amplitude coupling (see Materials and Methods and Tort et al., 2010b for details). **B**, Power spectral density in dB scale. Notice theta peak and absence of power peaks above 100 Hz. Inset shows power of fast oscillations in absolute scale (mV^2/Hz). **C**, Multiunit activity as a function of SLHFO phase. **D**, Left, mean SLHFO amplitude (top) and multiunit activity (bottom) as a function of theta phase. Right, Normalized SLHFO and multiunit activity versus theta phase (0, minimal activity; 1, maximal activity). **E**, LFP averages triggered by SLHFO peaks (top) and spike times (bottom). Dashed line represents trigger time. The results shown in this figure were obtained from a representative LFP recorded from CA1 stratum pyramidale in a freely behaving rat during active waking.

location in the CA1-DG axis was assessed by standard electrophysiological signatures (Fig. 3D, left). Current source density (CSD) was obtained by $-A + 2B - C$ for adjacent sites.

We focused our analysis on periods of high theta activity (5–10 Hz) as identified by inspection of time–frequency analysis of LFP power.

Results

Comodulation maps computed for LFPs recorded from the CA1 pyramidal layer typically exhibited coupling between theta phase and the amplitude of broadband high-frequency activity above 100 Hz (Fig. 1A). Based on results we show below, we refer to this type of high-frequency LFP activity as spike-leaked high-frequency oscillations (SLHFO). The power spectral density (PSD) of LFP recordings exhibiting prominent theta–SLHFO coupling (inferred by visual inspection of comodulation maps) typically exhibited peaks in theta and its first harmonic, but no power peaks above 100 Hz (Fig. 1B). Notice therefore that CFC analyses can reveal LFP activity that is not apparent in standard Fourier-based tools (Tort et al., 2008). Further analyses showed that SLHFO phase strongly modulates spike times (Fig. 1C). The unusual high levels of spike–field coupling, along with the absence of a true oscillatory activity in the PSD level, suggested to us that SLHFOs may be the remnants of extracellular action potentials in the LFP. If this is the case, we reasoned that the theta phase of maximal spiking activity and that of maximal SLHFO amplitude should match. This is precisely what we found for LFP recordings exhibiting prominent theta–SLHFO coupling in which SLHFO amplitude was maximal near the trough of theta wave, coinciding with the preferred theta phase of maximal multiunit activity (Fig. 1D). This result was further confirmed by analyzing LFP averages triggered by either spike times or the peaks of SLHFO, two approaches that typically provided quite similar results (a “spikelet” near the trough of the theta wave; Fig. 1E). Altogether, the results indicate that the coupling of theta phase and SLHFO amplitude apparent in the comodulation maps represents coupling between theta and spiking activity. These observations are consistent with

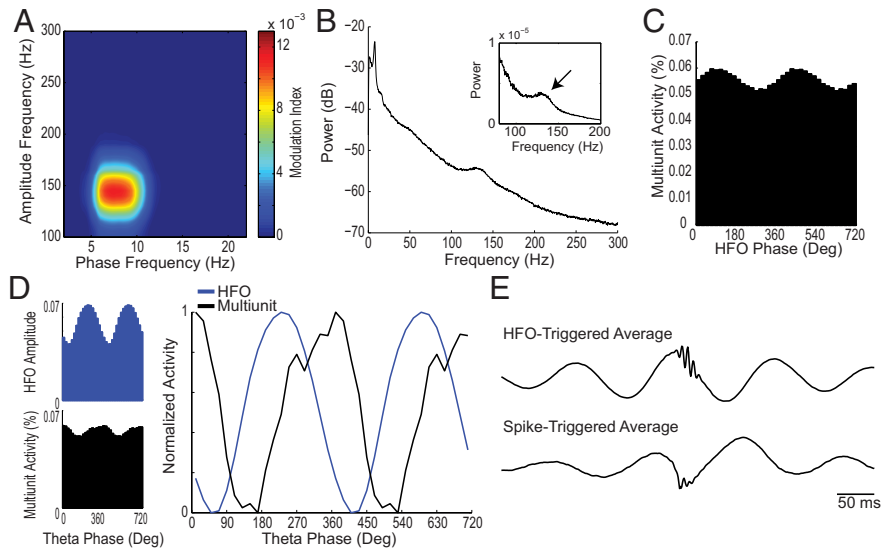


Figure 2. Theta phase modulates genuine high-frequency oscillations >100 Hz in the hippocampus. **A**, Comodulation map. **B**, Power spectral density in dB scale. Notice theta peak and a power peak \sim 140 Hz. Inset shows power of fast oscillations in absolute scale (mV^2/Hz). **C**, Multiunit activity as a function of HFO phase. **D**, Left, Mean HFO amplitude (top) and multiunit activity (bottom) as a function of theta phase. Right, Normalized HFO and multiunit activity vs theta phase. **E**, LFP averages triggered by HFO peaks (top) and spike times (bottom). The results shown in this figure were obtained from a representative LFP recorded from CA1 stratum oriens-alveus in a freely behaving rat during active waking.

recent findings suggesting that high-frequency LFP activity represents spike contamination into lower frequencies (see Introduction).

However, we saw a different picture when applying the same CFC framework to electrodes located above the pyramidal layer, in CA1 stratum oriens-alveus. The comodulation maps in these cases revealed coupling between theta and the amplitude of a different type of high-frequency LFP activity, which was rather circumscribed between 110 and 160 Hz (Fig. 2A). We refer to this type of LFP activity as HFO. The PSD of LFPs exhibiting prominent theta–HFO coupling displayed a power peak around 140 Hz (Fig. 2B); contrary to SLHFO, therefore, this analysis shows that HFOs are genuine LFP oscillations. HFO phase modulated multiunit activity, but to a much lower extent than what was found for SLHFO (compare Fig. 1C and Fig. 2C). To demonstrate that HFOs are not a byproduct of spectral contamination from spiking activity, it would be sufficient to show that the theta phase of maximal HFO amplitude differs from that of spikes. Accordingly, HFO amplitude was maximal at the descending phase of the theta cycle, considerably preceding the preferred phase of spikes (Fig. 2D). LFP averages confirmed the different phases between maximal HFO and spike activity (Fig. 2E). Of note, HFO-triggered averages exhibited fast oscillations riding on the descending phase of slower theta oscillations and not a spikelet as in the case of SLHFO (see Kramer et al., 2008). In all, these observations show that theta phase modulates genuine LFP oscillations above 100 Hz, which are not artifacts of spike contamination.

HFO and SLHFO are maximally coupled to theta above and at the pyramidal cell layer, respectively. Interestingly, comodulation maps of LFPs recorded just above the pyramidal layer exhibited both theta–SLHFO and theta–HFO coupling, along with an HFO peak in the PSD (Fig. 3A). These recordings directly confirmed the different theta phases of maximal HFO and SLHFO amplitude, with the latter coinciding with the units (Fig. 3B,C). Thus, both genuine and spurious high-frequency LFP activity above 100 Hz can occur in a same brain region. LFP recordings from a 16-site probe spanning the CA1–DG axis further con-

firmed HFO and SLHFO peak activity at the descending theta phase and at the theta trough, respectively (pyramidal layer reference; Fig. 3D). SLHFO did not exhibit any phase reversal across hippocampal layers, and CSD analysis revealed prominent SLHFO sink-source pairs at stratum pyramidale (Belluscio et al., 2012). Surprisingly, although HFO characteristically appear modulated by theta above the pyramidal layer (Scheffer-Teixeira et al., 2012), HFO phase reversed in DG, where CSD indicated the presence of sink-source pairs (Fig. 3D).

Finally, in Figure 4 we present group data of the theta phase distribution of SLHFO, HFO, and CA1 multiunit activity (Fig. 4A) and of the preferred theta phase of peak activity (Fig. 4B). Mean theta phase of peak activity was statistically different between HFO and both SLHFO and multiunit activity ($*p < 0.0001$; Watson–Williams test, $F_{(2,492)} = 523.14$), but not between SLHFO and multiunit activity ($p = 0.49$, $F_{(1,363)} = 0.48$).

Discussion

Here we have used a CFC approach to demonstrate that LFP activity above 100 Hz can denote either the spectral leakage from extracellular spikes or the presence of genuine network oscillations, or even both phenomena simultaneously. In particular, CFC analyses revealed that the theta phase of maximal multiunit activity may or may not coincide with that of maximal high-frequency LFP activity.

Consistent with previous reports (Ray et al., 2008c; Manning et al., 2009; Jia and Kohn, 2011), we showed that broadband increases in high-frequency LFP activity, usually called high-gamma in the human and monkey literature (Canolty et al., 2006; Ray et al., 2008a; Ray et al., 2008b), can be related to multiunit activity. In fact, we concluded that coupling between theta phase and the amplitude of SLHFO that appears in some comodulation maps essentially reflects coupling between theta oscillations and spike times. In accordance with this conclusion, using the hippocampal pyramidal layer as reference, peak spiking activity at the population level occurs near the theta trough (Buzsáki et al., 1983; Csicsvari et al., 1999), which is the same phase of maximal SLHFO amplitude (Fig. 1 and Fig. 3). In addition, the comodulation map further corroborated the broadband nature of spike-leaked activity in the LFP (Fig. 1A), a conclusion previously reached by standard power spectral analyses (Manning et al., 2009; Miller, 2010; Ray and Maunsell, 2011). It should be stressed that we regard as spurious the very high modulation of spiking activity by SLHFO phase shown in Figure 1C; notice that this spike–phase coupling is even higher than that found for theta phase. We interpret SLHFO as “leftovers” (or “scars”) of action potentials in the field potential; in this sense, as remnants of local spikes, it is expected that the spike waveforms strongly modulate their associated spike times.

Apart from the well accepted hippocampal ripple oscillations (Ylinen et al., 1995), it is currently believed that broadband high-frequency LFP activity essentially denotes spiking activity (see

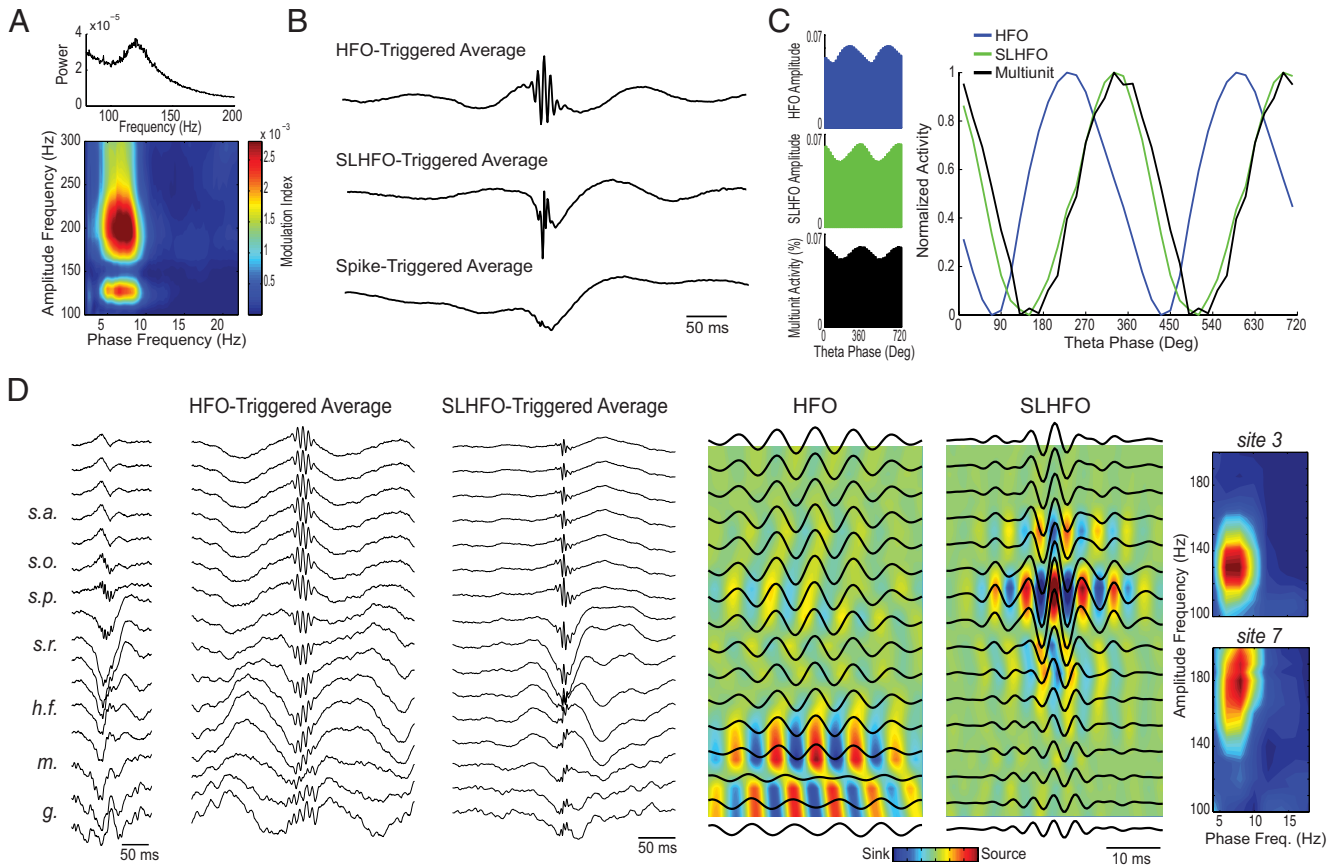


Figure 3. Theta phase can simultaneously modulate genuine and spurious high-frequency oscillations. **A**, Top, Power spectral density (in mV^2/Hz). Bottom, Comodulation map. **B**, LFP averages triggered by the peaks of HFO (top) and SLHFO (middle), and by spike times (bottom). **C**, Left, Mean HFO amplitude (top), SLHFO amplitude (middle), and multiunit activity (bottom) as a function of theta phase. Right, Normalized HFO, SLHFO, and multiunit activity versus theta phase. The results in **A–C** were obtained from a representative LFP recorded near CA1 stratum pyramidale in a freely behaving rat during active waking. **D**, First column, representative sharp wave ripple event recorded from a 16-site probe (100 μm spacing); second and third columns, LFP averages triggered by the peaks of HFO (reference, site 1) and SLHFO (reference, site 7); fourth and fifth columns, averaged HFO- and SLHFO-filtered LFPs (same trigger as before); the color plots show the associated CSD maps; sixth column, comodulation maps for a recording site above (top) and (bottom) at the pyramidal layer. Notice prominent theta-HFO and theta-SLHFO coupling, respectively.

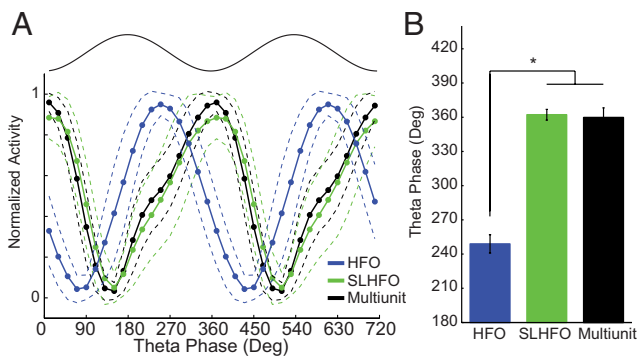


Figure 4. Group results. **A**, Mean normalized HFO, SLHFO, and multiunit activity as a function of theta phase (pyramidal layer reference). Theta peaks and troughs correspond to 180° and 360°, respectively (top sinusoid). These averages were computed from the pool of all electrodes exhibiting theta-HFO ($n = 129$) or theta-SLHFO ($n = 182$) coupling, as assessed by visual inspection of comodulation maps, across rats and behavioral sessions. Multiunit activity was obtained from multisite shanks placed at the pyramidal layer using each electrode contact as reference. Dashed lines denote the mean \pm 1 SD. **B**, Mean theta phase of peak activity; * $p < 0.0001$ (Watson-Williams test). Error bars denote 99% confidence intervals.

Introduction). Here we challenge this interpretation by showing another type of genuine high-frequency activity above 100 Hz. Similar high-frequency oscillations of ~ 140 Hz appear in several regions of motor circuits under systemic NMDA receptor block-

ade (Hunt et al., 2006; Nicolás et al., 2011), but whether they correspond to the same HFOs as the ones observed here is unclear. The biophysical mechanisms underlying physiological theta-associated HFO remain to be established (for a review, see Tort et al., 2013).

The main findings distinguishing genuine LFP oscillations above 100 Hz (HFO) from spike-leaked activity (SLHFO) were: (1) the circumscribed nature of HFO in the comodulation maps as opposed to the broadband activity of SLHFO; (2) the presence of a clear power peak above 100 Hz in the PSD of LFPs exhibiting prominent theta-HFO coupling; in contrast, there was no power peak above 100 Hz in LFP traces exhibiting only theta-SLHFO coupling; (3) the different theta phases of peak activity, with HFO and SLHFO having maximal amplitude at the descending phase and near the theta trough, respectively; (4) the presence of genuine oscillations in the LFP averages triggered by HFO amplitude peaks, but not when SLHFO activity is used as the trigger; (5) finally, in contrast to SLHFO, HFO modulation of spiking activity is considerably smaller (Fig. 2C) and comparable in strength to that found for other LFP rhythms such as gamma oscillations (Colgin et al., 2009). Overall, we conclude that theta-associated HFOs are not caused by contamination of the LFP signal by extracellular action potentials.

Belluscio et al. (2012) have recently defined “fast gamma”—or epsilon (ϵ) band—as LFP activity between 90–140 Hz, an overlap-

ping frequency range with the HFOs studied here. Nevertheless, the fast gamma oscillations investigated in Belluscio et al. (2012) peaked near the trough of the theta wave during active waking. Moreover, they also found a shift in the preferred theta phase of maximal activity from the awake state to REM sleep, which occurred for both fast gamma and spiking activity (Belluscio et al., 2012). This contrasts to the stability of the preferred HFO coupling phase across vigilance states (after the theta peak in both active waking and REM sleep; Scheffzük et al., 2011). Finally, Belluscio et al. (2012) found maximal theta-fast gamma coupling in stratum pyramidale, while hippocampal theta-HFO coupling is maximal in stratum oriens-aleveus (Scheffer-Teixeira et al., 2012). We thus speculate that the fast gamma oscillations studied in Belluscio et al. (2012) originated from spike contamination, i.e., they would correspond to SLHFO and not be a genuine rhythm. Notice therefore that although SLHFO activity is most prominent at frequencies higher than 150 Hz, it is important to realize that in the absence of genuine fast oscillations, such as gamma and HFO, the remnants of spiking activity can leak into much lower frequencies (down to 50 Hz according to some authors; Ray and Maunsell, 2011). For example, the HFO-filtered signal of the LFP examined in Figure 1 also has maximal amplitude at the same theta phase as the multiunit activity (data not shown). This is because there is no genuine oscillatory activity in the HFO range in this case; filtering the LFP at the HFO band (110–160 Hz) still largely reflects the spectral leakage of spiking activity. Therefore, we conclude that there is no exact definition for a frequency range that can separate genuine from spurious high-frequency LFP oscillations per se. These observations suggest that whether high-gamma activity in field potentials reflects a true rhythm or spike contamination should be examined on a case-by-case basis.

In summary, our results as well as results from other groups indicate that special attention should be given to possible influences of extracellular spikes when studying fast oscillations in field potential. Conversely, recent work conveyed the idea that high-frequency LFP activity is essentially due to spiking activity (Ray et al., 2008b; Jia and Kohn, 2011; Ray and Maunsell, 2011; Buzsáki et al., 2012), but the HFOs constitute a compelling counterexample to this generalization. In all, these findings add to others (Kopell et al., 2010; Tort et al., 2010a) that recommend avoiding defining brain rhythms solely based on frequency ranges.

Notes

Supplemental material for this article is available at <http://www.jneurosci.org> featuring a MATLAB toolbox for computing phase–amplitude coupling. This material has not been peer reviewed.

References

- Belluscio MA, Mizuseki K, Schmidt R, Kempter R, Buzsáki G (2012) Cross-frequency phase–phase coupling between θ and γ oscillations in the hippocampus. *J Neurosci* 32:423–435. [CrossRef Medline](#)
- Buzsáki G, Wang XJ (2012) Mechanisms of gamma oscillations. *Annu Rev Neurosci* 35:203–225. [CrossRef Medline](#)
- Buzsáki G, Leung LW, Vanderwolf CH (1983) Cellular bases of hippocampal EEG in the behaving rat. *Brain Res* 287:139–171. [Medline](#)
- Buzsáki G, Anastassiou CA, Koch C (2012) The origin of extracellular fields and currents—EEG, ECoG, LFP and spikes. *Nat Rev Neurosci* 13:407–420. [CrossRef Medline](#)
- Canolty RT, Edwards E, Dalal SS, Soltani M, Nagarajan SS, Kirsch HE, Berger MS, Barbaro NM, Knight RT (2006) High gamma power is phase-locked to theta oscillations in human neocortex. *Science* 313:1626–1628. [CrossRef Medline](#)
- Colgin LL, Denninger T, Fyhn M, Hafting T, Bonnevie T, Jensen O, Moser MB, Moser EI (2009) Frequency of gamma oscillations routes flow of information in the hippocampus. *Nature* 462:353–357. [CrossRef Medline](#)
- Crone NE, Sinai A, Korzeniewska A (2006) High-frequency gamma oscillations and human brain mapping with electrocorticography. *Prog Brain Res* 159:275–295. [CrossRef Medline](#)
- Csicsvari J, Hirase H, Czurkó A, Mamiya A, Buzsáki G (1999) Oscillatory coupling of hippocampal pyramidal cells and interneurons in the behaving rat. *J Neurosci* 19:274–287. [Medline](#)
- Delorme A, Makeig S (2004) EEGLAB: an open source toolbox for analysis of single-trial EEG dynamics including independent component analysis. *J Neurosci Methods* 134:9–21. [CrossRef Medline](#)
- Freeman WJ (2007) Definitions of state variables and state space for brain-computer interface: Part 1. Multiple hierarchical levels of brain function. *Cogn Neurodyn* 1:3–14. [CrossRef Medline](#)
- Hunt MJ, Raynaud B, Garcia R (2006) Ketamine dose-dependently induces high-frequency oscillations in the nucleus accumbens in freely moving rats. *Biol Psychiatry* 60:1206–1214. [CrossRef Medline](#)
- Jacobs J, Manning J, Kahana M (2010) Response to Miller: “Broadband” vs. “high gamma” electrocorticographic signals. *J Neurosci* 30, online.
- Jia X, Kohn A (2011) Gamma rhythms in the brain. *PLoS Biol* 9:e1001045. [CrossRef Medline](#)
- Kopell N, Kramer MA, Malerba P, Whittington MA (2010) Are different rhythms good for different functions? *Front Hum Neurosci* 4:187. [CrossRef Medline](#)
- Kramer MA, Tort AB, Kopell NJ (2008) Sharp edge artifacts and spurious coupling in EEG frequency comodulation measures. *J Neurosci Methods* 170:352–357. [CrossRef Medline](#)
- Manning JR, Jacobs J, Fried I, Kahana MJ (2009) Broadband shifts in local field potential power spectra are correlated with single-neuron spiking in humans. *J Neurosci* 29:13613–13620. [CrossRef Medline](#)
- Miller KJ (2010) Broadband spectral change: evidence for a macroscale correlate of population firing rate? *J Neurosci* 30:6477–6479. [CrossRef Medline](#)
- Miller KJ, Zanos S, Fetz EE, den Nijs M, Ojemann JG (2009) Decoupling the cortical power spectrum reveals real-time representation of individual finger movements in humans. *J Neurosci* 29:3132–3137. [CrossRef Medline](#)
- Mizuseki K, Sirota A, Pastalkova E, Buzsáki G (2009) Theta oscillations provide temporal windows for local circuit computation in the entorhinal-hippocampal loop. *Neuron* 64:267–280. [CrossRef Medline](#)
- Nicolás MJ, López-Azcárate J, Valencia M, Alegre M, Pérez-Alcázar M, Iriarte J, Artieda J (2011) Ketamine-induced oscillations in the motor circuit of the rat basal ganglia. *PLoS One* 6:e21814. [CrossRef Medline](#)
- Peyrache A, Battaglia FP, Destexhe A (2011) Inhibition recruitment in prefrontal cortex during sleep spindles and gating of hippocampal inputs. *Proc Natl Acad Sci U S A* 108:17207–17212. [CrossRef Medline](#)
- Ray S, Maunsell JH (2011) Different origins of gamma rhythm and high-gamma activity in macaque visual cortex. *PLoS Biol* 9:e1000610. [CrossRef Medline](#)
- Ray S, Niebur E, Hsiao SS, Sinai A, Crone NE (2008a) High-frequency gamma activity (80–150 Hz) is increased in human cortex during selective attention. *Clin Neurophysiol* 119:116–133. [CrossRef Medline](#)
- Ray S, Hsiao SS, Crone NE, Franaszczuk PJ, Niebur E (2008b) Effect of stimulus intensity on the spike-local field potential relationship in the secondary somatosensory cortex. *J Neurosci* 28:7334–7343. [CrossRef Medline](#)
- Ray S, Crone NE, Niebur E, Franaszczuk PJ, Hsiao SS (2008c) Neural correlates of high-gamma oscillations (60–200 Hz) in macaque local field potentials and their potential implications in electrocorticography. *J Neurosci* 28:11526–11536. [CrossRef Medline](#)
- Scheffer-Teixeira R, Belchior H, Caixeta FV, Souza BC, Ribeiro S, Tort ABL (2012) Theta phase modulates multiple layer-specific oscillations in the CA1 region. *Cereb Cortex* 22:2404–2414. [CrossRef Medline](#)
- Scheffzük C, Kukushka VI, Vyssotski AL, Draguhn A, Tort AB, Brankačk J (2011) Selective coupling between theta phase and neocortical fast gamma oscillations during REM-sleep in mice. *PLoS One* 6:e28489. [CrossRef Medline](#)
- Tort ABL, Kramer MA, Thorn C, Gibson DJ, Kubota Y, Graybiel AM, Kopell NJ (2008) Dynamic cross-frequency couplings of local field potential oscillations in rat striatum and hippocampus during performance of a T-maze task. *Proc Natl Acad Sci U S A* 105:20517–20522. [CrossRef Medline](#)
- Tort ABL, Fontanini A, Kramer MA, Jones-Lush LM, Kopell NJ, Katz DB (2010a) Cortical networks produce three distinct 7–12 Hz rhythms dur-

- ing single sensory responses in the awake rat. *J Neurosci* 30:4315–4324. CrossRef Medline
- Tort ABL, Komorowski R, Eichenbaum H, Kopell N (2010b) Measuring phase-amplitude coupling between neuronal oscillations of different frequencies. *J Neurophysiol* 104:1195–1210. CrossRef Medline
- Tort ABL, Scheffer-Teixeira R, Souza BC, Draguhn A, Brankačk J (2013) Theta-associated high-frequency oscillations (110–160Hz) in the hippocampus and neocortex. *Prog Neurobiol* 100:1–14. CrossRef Medline
- Ylinen A, Bragin A, Nádasdy Z, Jandó G, Szabó I, Sik A, Buzsáki G (1995) Sharp wave-associated high-frequency oscillation (200 Hz) in the intact hippocampus: network and intracellular mechanisms. *J Neurosci* 15:30–46. Medline